Paleoecology and proliferation of the bivalve *Chondrodonta joannae* (Choffat) in the upper Cenomanian (Upper Cretaceous) Adriatic Carbonate Platform of Istria (Croatia)

DOI: 10.1016/j.palaeo.2020.109703

Renato Posenato[1*], Gianluca Frijia[1], Michele Morsilli[1], Alan Moro[2], Gabriella Del Viscio[1], Aleksandar Mezga[2]

1-Dipartimento di Fisica e Scienze della Terra, Università di Ferrara, Via Saragat 1, 44121 Ferrara, Italy.

2- University of Zagreb, Faculty of Science, Department of Geology, Horvatovac 102a, 10000 Zagreb, Croatia.

*Corresponding author. E-mail address: Renato Posenato, psr@unife.it; Gianluca Frijia, frjglc@unife.it; Michele Morsilli, mrh@unife.it; Alan Moro, amoro@geol.pmf.hr; Gabriella Del Viscio, dlvgrl@unife.it; Aleksandar Mezga, amezga@geol.pmf.hr

ABSTRACT

Chondrodonta joannae (Choffat) is a morphologically variable oyster-like bivalve with a predominately calcitic shell. An exceptional exposure of *C. joannae*-bearing strata of late Cenomanian age crops out along the seaside in northern Istria (Croatia) and permits a taphonomical and functional analysis in order to define the life habit and growth strategies of this bivalve. The *C. joannae* population from the studied succession is characterised by highly-elongated, large and curved shells, reaching about 50 cm in height and 5 cm in length. This shell shape is typical of the club-like bivalve morphotype, which was adapted to soft-bottom substrates with high sediment accumulation. The shell is slightly inequivalve and characterized by a reduced body cavity, a few centimetres high, and a dorsal region up to 10 times longer. The shell opening mechanism was mostly based on the resilium located between the chondrophores which protrude in the body cavity. The abandoned dorsal cavity is filled by a calcite hinge plate, the ventral edge of which acted as fulcrum for the valve flexibility. In the hinge plate, the function of chondrophores changed. They acted as a hinge to keep tightly interlocked the valves, which considerably emerged above the sediment-water interface. The individuals were arranged in low shrub-type congregations, which produced low-relief mounds. The functional morphology and taphonomic signature suggest that *C. joannae* individuals collected food at a greater distance from the bottom with respect to the co-occurring rudists. We speculate that the *C. joannae* proliferation could be related to a late Cenomanian phase of environmental instability predating the OAE2 with fluctuating climatic conditions and ocean fertility.

Key-words: taphonomy, functional morphology, epifaunal tiering, rudists, OAE 2.

1. Introduction

On the shallow water carbonate platforms of the Cretaceous, bivalves experienced a great proliferation and an extraordinary adaptive radiation (Steuber et al., 2016 and references therein). The most peculiar and famous Cretaceous bivalves are represented by the rudists, a group characterized by aberrant shell morphologies, ranging from club- to horn-like shells, which allowed them to occupy several ecological niches of level-bottom environment (e.g., Skelton, 2018). Rudist biodiversity shows three radiation phases, each of them was followed by an extinction event (Ross and Skelton, 1993). The first two extinctions occurred in the early Aptian and latest Cenomanian, in correspondence with severe Cretaceous paleoenvironmental-paleoclimatic perturbations (e.g., Anoxic Events 1a and 2; Philip and Airaud-Crumiere, 1991; Gili et al., 1995; Skelton and Gili, 2002; Masse and Steuber, 2007; Steuber et al., 2016; Skelton, 2018, Frijia et al., 2019).

Rudist communities may have been composed either by hard and soft bottom dwellers, the latter sometimes becoming the dominant forms. One of the most common bivalve occurring in the rudist-bearing limestone is *Chondrodonta*, which developed a "mud-sticker" strategy of bottom stabilization (e.g., Ayoub-Hannaa and Fürsich, 2011) similar to the rudist elevator ecological morphotypes (e.g., radiolitids and hippuritids; Skelton and Gili, 2002). *Chondrodonta* is an oyster-like bivalve with a predominantly calcitic and dorso-ventrally elongated shell. This genus has been considered an opportunistic taxon which shows a discontinuous distribution in the Barremian to Campanian (?) carbonate platforms from the Middle East to Caribbean Tethyan bioprovinces (Dhondt and Dieni, 1992, 1993). During the early evolutionary phase, in the early Aptian, *Chondrodonta* was of characteristically small sized and with prevailing smooth shells with a short hinge plate. These characters distinguished *C. glabra* Stanton, which in the Gargano Promontory (southern Italy) created meter-thick accumulations located stratigraphically below the onset of the OAE 1a (Graziano, 2013; Graziano et al., 2013; Guerzoni, 2016; Posenato et al., 2018). This species developed a "mud-sticker" bottom stabilization and produced moderately elongated, stick-like shells (Posenato et al., 2018).

78 *Chondrodonta* is also very abundant in the Late Cretaceous, mostly represented by large and
79 plicated shells belonging to *C. joannae* (Choffat). This species, restricted to the late Cenomanian, is
80 characterized by a large shell with considerably morphological variability, for instance, ranging
81 from elongate-ovate to fan-shaped forms (Dhondt and Dieni, 1993). For the case of the Late
82 Cretaceous Adriatic Carbonate Platform, this species produced thick and widespread shell
83 accumulations, which are used as a regional marker bed (e.g., Polšak, 1967a; Gušić and Jelaska,
84 1993; Jurkovšek et al., 1996).
85 The northern rocky coast of Cape Savudrija area (Fig. 1) shows a spectacular outcrop of
86 *Chondrodonta*-bearing limestones which have been documented since the early 20th century
87 (Schubert, 1903), Here, *C. joannae* developed extremely aberrant shells, with a typical club-like
88 morphology, reaching ~50 cm in height. This morphology is very similar to that of the best known
89 extinct stick-like bivalves, such as the Lower Jurassic *Lithiotis* (e.g., Chinzei, 1982; Posenato and
90 Masetti, 2012; Brandolese et al., 2019), the Cretaceous oyster *Konbostrea*, and the elevator rudists
91 (e.g., Chinzei, 1986, 2013; Skelton and Gili, 2002). These taxa, which belong to different
92 evolutionary lineages, developed strongly elongated shells adaptive for occupying soft-bottom
93 substrates subjected to high rates of sedimentation To avoid gill suffocation, the body cavity raised
94 from the sediment-bottom interface, abandoning the dorsal/umbonal shell, which was filled by
95 chalky carbonates or chambered. The burial of most part of the shell imposed opening and closing
96 mechanisms based on shell elasticity or vertical movements of the upper lid-like valve (Seilacher,
97 1984; Chinzei, 1986, 2013). Shell morphology, life habit and growth strategies of *C. joannae* from
98 the upper Cenomanian Cape Savudrija succession are here analysed and compared to other club-
99 like bivalves. Finally, we will discuss the late Cenomanian proliferation of *C. joannae* and the
100 *Chondrodonta*-rudist ecological competition.
101
102 **2. Geological setting**
103

104 The study area is located in the north-western part of the Istrian Peninsula (Croatia) close to
105 the national border between Croatia and Slovenia (Fig. 1A). The succession crops out along the
106 rocky coast in the NW-SE elongated promontory of Savudrjia area (Fig. 1C).
107 The carbonate successions of the Istrian Peninsula belongs to the Adriatic Carbonate
108 Platform (AdCP), which was one of the largest Mesozoic carbonate platforms of the Peri-
109 Mediterranean region, which developed as an isolated platform during the rifting phase that
110 dismantled and drowned the extensive Upper Triassic-Lower Jurassic platform with the creation of
111 a series of basinal areas such as the Adriatic/Belluno Basin, which borders the AdCP to the west
112 (e.g., Winterer and Bosellini, 1981; Zappaterra, 1994; Tišljar et al., 2002; Velić et al., 2003;
113 Vlahović et al., 2005; Cazzini et al., 2015; Wrigley et al., 2015). The drifting phase, related to the
114 opening of the Alpine Tethys, created a broad passive margin and the AdCP experienced a general
115 thermal subsidence, resulting in the formation of a thick stack of shallow-water carbonate sediments
116 (up to 8 km, Brčić et al., 2017) from the Jurassic until the Eocene time (Tišljar et al., 2002;
117 Vlahović et al., 2005). The shallow-water carbonate sedimentation was interrupted, mostly during
118 the Cretaceous, by several periods of sub-aerial exposure, as well as drowning events, such as
119 during the Turonian interval (Jenkyns, 1991; Moro, 1997; Davey and Jenkyns, 1999; Moro et al.,
120 2002; Vlahović et al., 2005; Korbar et al., 2012), as a consequence of combined synsedimentary
121 tectonics and eustasy (Gušić and Jelaska, 1990, 1993; Herak, 1991; Moro et al., 2002; Vlahović et
122 al., 2005). The passive margin stage ended with the onset of the Alpine collision in the Paleogene,
123 and consequently part of the AdCP, and particularly the Istrian Peninsula, start to act as the foreland
124 of the orogenic system with a regional flexure and uplift (forebulge) that create an extensive
125 emergence and karstification of the platform (Otoničar, 2007). With the SW migration of Dinaric
126 fold-and-thrust belt, the foreland basin started to subside, filling with flysch deposits accumulated in
127 the foredeep, atop the previously deposited carbonate successions (Fig. 1B) (Wrigley et al., 2015).
128 During the late Paleogene and Neogene, thrust and fold propagations created the actual structural
129 setting of the Istrian Peninsula (Márton et al., 2008, 2014; Korbar, 2009).

According to the stratigraphy and tectonic lineaments, the north-western part of the Istrian Peninsula can be divided in two main areas. The southern part is characterized by a broad and gentle anticline plunging toward NE (Fig. 1B) with at the nucleus shallow water carbonate of Late Jurassic in age, succeeded on both flanks by the whole Lower Cretaceous succession and some Cenomanian deposits. This regional trend is interrupted by a ENE-WSW oriented thrust, north of Umag, that create a parallel anticline structure, or thrust fold, forming the Savudrjia/Punta Salvore promontory (Fig. 1C). The northern part is occupied by extensive flysch deposits of Eocene age (Fig. 1B; e.g., Pleničar et al., 1969; Polšak and Šikić, 1969).

In the Savudrjia area, the stratigraphy is quite simple and formed by limestones of Albian and Cenomanian age. The sampled succession belongs to the upper Cenomanian shallow marine peritidal facies (Tišljar et al., 1983; Moro et al., 2007) and consists of subtidal wackestone-packstone/floatstones and intertidal-supratidal stromatolites (Polšak, 1965; 1967a; Dalla Vecchia et al., 2001; Mezga et al., 2006; Moro et al., 2007). The lower reaches of this unit are characterized by radiolitids, and scattered monopleurids, that occur as biostromes or dispersed in the lime mud sediments (Polšak, 1967a; Pleničar et al., 1969). The upper part of the Cenomanian limestones records a significant change in the bivalve associations, which become *Chondrodonta*-dominated (Fig. 2). So pronounced is this taxonomical change, that it has been used as the marker of the upper part of the Cenomanian of the Istrian peninsula (Polšak, 1965; 1967b; Magaš, 1968; Pleničar et al., 1969; Polšak and Šikić, 1969; Šikić et al., 1969, 1972), as well as the upper part of the Milna (Gušić and Jelaska, 1990) and Povir formations (Jurkovšek et al., 1996) within the Upper Cretaceous lithostratigraphic division of AdCP.

The studied section is 42.5 m thick and consists of three main intervals (Fig. 2). The first of these (0 to 12 m from the base of the section) is comprised of wacke- to grainstone alternating with scatter-laminated packstone-grainstone and bindstone with *Thaumatoporella parvoversiculifera* and benthic foraminifera as well as wackestone-floatstone with rudist shells (radiolitids and rare monopleurids). The second interval, meanwhile (12 to 26 m from base), is characterised by wacke-

156 to grainstone with benthic foraminifera grading to closely-spaced beds of floatstone-rudstone,
157 predominantly composed by rudists and *Chondrodonta* shells. Bindstone is rare, but when
158 observed, is presented with clotted fabric and fenestrae. A major exposure surface marks the top of
159 this interval. The last part of the section, from 26 to 42.5 meters, is characterised by an alternation
160 of float- to rudstone, locally boundstone, dominated by *Chondrodonta* shells with *Thaumatoporella*
161 and wackstone to rare grainstone with benthic foraminifera. This facies association can be
162 interpreted as a typical inner-platform setting (Moro et al., 2007). The platform margin, visible in
163 offshore seismic profiles, is less than 15 km westward of the Cape Savudrija tip (Grandić et al.,
164 2013; Velić et al., 2015).
165 The occurrence, from the base to the top of the considered section, of *Chrysalidina gradata*
166 D'Orbigny, *Pastrikella balcanica* (Cherchi, Radoičić and Schroeder), *Vidalina radoicicae* Cherchi
167 and Schroeder, *Pseudorhapydionina dubia* (De Castro), and *Pseudolituonella reicheli* Marie (Fig.
168 2) allows for correlation the section to the *V*. *radoicicae-C*. *gradata* concurrent range zone of Velić
169 (2007) of the Upper Cretaceous deposits of the Adriatic Carbonate Platform and the lower part of
170 the *C*. *gradata-P*. *reicheli* biozone of Chiocchini et al. (2012) of the central Apennine Carbonate
171 Platform, both suggesting the middle-upper part of the upper Cenomanian. This dating is confirmed
172 by isotope stratigraphy, which places the top of the *C*. *gradata-P*. *reicheli* biozone into the
173 uppermost Cenomanian (Frijia et al., 2015).
174
175 3**. Materials and methods**
176
177 The present study is based on a several hundred shells observed and photographed in the
178 field and on twenty specimens analysed in the laboratory. Four shells have been sectioned
179 perpendicularly to the commissural plane, both in antero-posterior and dorso-ventral directions in
180 order to reconstruct their internal morphology. The serial sections have then been polished, and
181 acetate peels made. These peels were subsequently scanned with an optical scanner at 1200 dpi. The

studied material will be kept in the paleontological collection of the Department of Geology, Faculty of Science, University of Zagreb.

4. Taphonomy

4.1. Biostratinomy

In outcrop, the *C. joannae* accumulations often show large exposures on the bed-plane surface with a high rate of shell coverage rate. The completeness of the shells is variable, but not to the point that there is clear evidences of transport and reorientation by prevailing current orientations. These observation intimate that the considered accumulations are para- to authochtonous. Field evidences (Fig. 1E) indicate, for *C. joannae*, a depositional model similar to that proposed for the lower Aptian *C. glabra* accumulations from the Gargano Promontory which consists of a narrow core with shells in life position, and wide flanks with parauthochtonous and broken valves. In the upper Cenomanian succession of Cape Savudrija, *C. joannae* created shell accumulations together with pectinoids (e.g., *Neithea*) and sparse rudists, mainly represented by radiolitids, often aggregated in bouquets, and rare individuals of monopleurids.

The most spectacular *C. joannae* accumulation, with a surface of about 5 m^2, occurs at 34.5 m from the base of the section (bed R21, Fig. 2). Complete and very large shells of *C. joannae* dominate over small sized and broken individuals, suggesting a congregation of several generations of the bivalve, with a low juvenile mortality (Fig. 3). The shells are generally curved, with radius of curvature often higher in the umbonal extremity, which imparts a hook-shape to this region of shells. Here, no individual is found in living position, but the occurrence of a few clusters composed of very elongated individuals suggest that the burial of *C. joannae* bouquets was rapid and with the absence of significant shell re-orientation by virtue of waves or currents. The random distribution of the shells is supported by the rose diagrams capturing their growth directions of multiple

individuals observed on the surface (Fig. 3.3) and for separated areas of the same surface (Fig. 3.4a-d). The high population density of *C. joannae* can be related to the gregariousness of larval settlement, as is also observed in living oysters (e.g., Chinzei, 2013). In the Cape Savudrija succession, only small-sized shells have been found in upright position, while the large individuals always lie in a toppled position, contrary to their living position as suspension feeding bivalves.

4.2. Diagenesis

Only the calcitic parts of the *Chondrodonta* shells are preserved. These parts encompass the outer shell layers, chondrophores and hinge plate. The dissolution of the inner aragonitic layers occurred during an early diagenetic phase when the sediment was not fully indurated. The occurrence and rapid dissolution of an inner aragonite layer is supported by the moulds, reproduced on the muddy matrix, of the inner surface of the calcite layer, where pseudo-growth lines are visible due to the dissolution of the inner shell layer (Fig. 4). Aragonite dissolution caused the loss of internal features such as the muscle scar and pallial line, and probably also of some components of the chondrophores (Fig. 5). Aragonite dissolution reduced the thickness and robustness of the shells and caused a strong compaction, particularly in those specimens laying with the commissural plane parallel to the bedding surface (e.g., Fig. 5.3). These shells are strongly flattened, the morphology of the hinge plate is distorted, hindering taxonomic identification. The space occupied by the aragonite is partially recognizable in specimens lying with the commissure plane perpendicular to bedding plane (e.g., Fig. 5.4) and by the presence of calcitic wedges which occur on the internal marginal ridges of the shells, which were interdigitate with the internal aragonitic layer.

5. The shell characteristics of *Chondrodonta joannae*

5.1. Shell orientation

234

235 The *Chondrodonta* shell was recognized by Stanton (1901, pl. 26, fig. 1) to consist of an attached,
236 possibly, left valve (considering the position of a supposed attachment scar in the umbonal region)
237 and a free valve. This orientation was also accepted by Douvillé (1902) and Cox and Stenzel
238 (1971). Freneix and Lefrèvre (1967), however, interpreted the attached valve as the right. This new
239 interpretation is supported by Dhondt and Dieni (1993; pl. 15, fig. 1-6) on the basis of the position
240 of the muscle scar preserved in some attached valves, who also confirmed the monomyarian
241 condition of the Chondrodontidae. The here studied specimens have been oriented according to
242 these latter authors. Therefore, the attached or lower valve is considered to be the right, while the
243 free or upper valve, is the left one.

244

245 *5.2. External characters*

246

247 The outline of the juvenile shells, which are up to 5 – 10 cm in height, is triangular to ovoid-
248 elongated. In its adult stage, the shell shows a compressed stick-like shape, reaching a maximum
249 height of about 50 cm and 4–5 centimetres in length (Fig. 6.11). In the large specimens, the shell
250 grew only in a ventral direction and therefore, the anterior and posterior margins are almost parallel.
251 The attachment scar is absent on examined specimens. This can be related to the bad preservation of
252 the beak in the observed specimens and the reduced extension of the scar surface. A cemented
253 behaviour of *Chondrodonta* during the juvenile stage is suggested by Dhondt and Dieni (1993) and
254 Posenato et al. (2018), and also observed in some bouquets from the Cape Savudrija succession
255 (Fig. 6.14). The absence of large shells in life position suggests a small and weak attachment scar,
256 which was unable to guarantee the stability of the individual on the seabed.

257 The umbonal region, which is a few cm high, often has a hook-like shape, which testifies to
258 a change in growth direction, possibly, related to the change of life habit (Figs 6.10–6.12). The
259 juvenile shell had a pleurothetic and cemented life habit, which is also recorded by the unequal

shape of the valves (inequivalve shell; Carter et al., 2012). The lower or right valve is more convex than the free or left valve (Fig. 7.3–9). During the ontogeny, the raising of the ventral region of the shell from the seabed generated variously curved commissure planes (Figs 6.11, 6.12). The original dorso-ventral curvature, related to the development of a curved life position, can be detected in those specimens buried with the commissure plane perpendicular or oblique to the bed surface (e.g., Fig. 6.12). In the shells lying with the commissure parallel to bedding surface, this curvature is obliterated by the sediment compaction (e.g., Figs 6.6–6.9). Some individuals also show lateral curvatures (e.g., Figs 6.1, 6.11), for others, a straight shell cannot be excluded. These observations suggest that the shell outline and shape had a high ecomorphic variability, likely related to the gregarious behaviour of very crowded populations, often arranged in bouquet-like congregations.

Shell ornamentation is also variable. The specimens are mostly radially plicated. They have one or two main median radial folds, with rounded apex extending from the beak to the ventral margin, branched on both sides in secondary folds, which in turn are irregularly bifurcated into short minor order folds. The robustness and density of folds is variable among individuals. The distance from adjacent crests, beyond ~5 cm from the apex, ranges from 3 mm to 10 mm. Densely and sparsely folded specimens are associated in the same bed (e.g., Figs 6.8, 6.9). In a few specimens, the ornamentation is mostly restricted to the dorsal region (Fig. 6.5). Others seem to be completely smooth (Fig. 6.1, 2). Growth lines are also variably developed. In some specimens, they originate a weak squamous ornamentation (e.g., Figs 6.5, 6.7).

5.3. Internal characters

The internal characters of the shells have been investigated in both disarticulated and articulated valves. These have been sectioned and observed in polished surfaces oriented anterior-posteriorly and perpendicularly to the commissure plane. In a shell of about 20 cm height, the body cavity is about 6 cm long (Fig. 7). The long dorsal part of the shell is massive and contains a thick hinge

286 plate, which fills the body space. In this specimen, the internal morphology is clearly detectable
287 because the shell has been scarcely affected by compaction. The chondrophores protrude ventrally
288 inside the body cavity for a length of about 10 mm (Figs 7.4, 7.5). The ventral projection of the
289 lower (or right) valve chondrophore is linguiform, having a tongue-like shape, displaying a
290 compressed ovoid shape in section, parallel to the commissural plane (Figs 5.1, 7,4). Here, the
291 ventral projection consists of calcitic homogeneous microstructure which is later enveloped by
292 foliated calcite (Fig. 5.3).
293 The chondrophore of the free (upper or left) valve consists of a ventrally-projected calcitic
294 plate, almost parallel to the commissural plane and protruding in the body cavity. In dorsal
295 direction, about 10 mm after the ventral extremity, the chondrophore becomes oblique and
296 cemented to the inner aragonitic layer, acquiring a hook-like shape (Figs 5.1, 7.4). At the dorsal
297 extremity of body cavity, this chondrophore is fused to the inner valve surface by sparry calcite,
298 which suggests an original aragonitic deposit (Fig. 5.1), which could represent the myostracum. The
299 anterior side is covered by foliated calcite, which is connected to the anterior marginal fold.
300 Therefore, the upper chondrophore becomes an antero-posteriorly curved ridge or blade cemented
301 to the inner aragonitic layer, running along the whole hinge plate until reaching the shell apex (e.g.,
302 Figs 7.6– 7.9).
303 The ventral part of the right (lower) chondrophore consists of a linguiform process with a
304 homogeneous microstructure projected inside the body cavity. It is dorsally enveloped by foliated
305 calcite, originating from an ovoid-compressed outline (Fig. 5.1). At the dorsal extremity of the body
306 cavity, the lower chondrophore is incorporated within a large and thick hinge plate of foliated
307 calcite which fills the body cavity. The hinge plate has a longitudinal anterior groove, which
308 represents the socket of the hook-like process of free valve in antero-posterior section (Figs 5.3–5.6,
309 8.4, 8.5, 9).
310 The hinge plate is connected to the anterior and posterior calcitic ridges and cemented to a
311 thin and irregular underlying sparry calcite layer (e.g., Fig. 5.4). The sparry calcite cement likely

312 precipitated within the voids produced by the dissolution of the aragonite. Therefore, the shape and
313 extension of the sparry calcite layer underlying the hinge plate are related to the degree of shell
314 compression and deformation.
315 The hinge plate surface is detectable in some eroded or disarticulated right valves (Fig. 8). In
316 the better preserved specimens, but with the chondrophores affected by diagenetic compaction, the
317 surface shows two parallel radial squared ridges and three shallow grooves (e.g., Fig. 8.10). The
318 posterior groove (G1) is flat and bears feebly and oblique growth lines (Fig. 8.10). The first ridge
319 (R1) is large and flattened at the top. The second groove (G2) is the largest and has a low and
320 smoothed radial bulge. The second ridge (R2) has a shape similar to the former. It is located above
321 the left chondrophore and is anteriorly limited by the recess (G3) receiving the hook-like process
322 (Fig. 5.6) or blade (Fig. 9.2) projecting from the inner surface of free valve (Figs 5.6, 7).
323 The growth lines detectable on the inner surface of the free valve have been originated by
324 the dissolution of the inner aragonitc layer (Fig. 4), while no evidence on the occurrence of an
325 aragonitic layer above the cardinal process has been observed.
326
327 *5.4. Classification*
328
329 *Chondrodonta* was tentatively placed by Stanton (1901, 1947) within the Pectinacea, while
330 Douvillé (1902), on the base of a supposed dimyarian condition, suggested a close relation with
331 Pinnidae. Other authors referred this genus to the Ostreida (e.g., Hoernes, 1902; Schubert, 1903;
332 Nevesskaja et al., 1971; Dhondt and Dieni, 1993; Bieler et al., 2010), or as "doubtful members" of
333 Ostreida (Cox and Stenzel, 1971; Carter, 1990). The affinity with oysters proposed by Dhondt and
334 Dieni (1993) was based on the occurrence of chomata in some *Chondrodonta* shells. However,
335 these structures are also present in the Plicatulidae (Carter et al., 2012).
336 Freneix and Lefévre (1967) proposed a close affinity of the family Chondrodontidae with
337 Plicatulidae and Prospondylidae because they are cemented on the right valve and without the

338 byssal attachment and share an oyster-like morphology. In the most recent classifications of the
339 Bivalvia Carter et al. (2011) placed Chondrodontidae within the superfamily Plicatuloidea (Order
340 Pectinida). This classification has been supported by recent observations on the shell composition
341 and microstructures (Posenato et al., 2018). The affinities with the living *Plicatula* are (1) the
342 cementation on the right valve, (2) the occurrence of an inner aragonitic layer, replaced in the fossil
343 shells by sparry calcite cement, and (3) an outer layer of simple and irregular complex crossed
344 foliated calcite. However, *Plicatula* and *Chondrodonta* show also significant differences, mostly
345 concerning the hinge and ligament morphologies.
346 The morphology of the hinge plate and chondrophores of *Chondrodonta* were used to divide
347 *Chondrodonta* into three subgenera (Freneix and Lefrèvre, 1967). *Chondrodonta* s.s. is
348 distinguished by a smooth hinge plate with *C. munsonii* (Hill) as type-species. This type of hinge
349 plate is also present in the Aptian *C. glabra* Stanton recorded from both Texas (Stanton, 1901,
350 1947) and Gargano Promontory (Posenato et al., 2018). *Chondrodonta* (*Cleidochondrella*) is
351 characterized by a double chondrophore of the attached valve with *C. elmaliensis* Freneix and
352 Lefrèvre as type-species (Santonian – Campanian in age). *Chondrodonta* (*Freneixita*) Stenzel (pro
353 *Chondrella* Freneix and Lefrèvre) is instead distinguished by a double elongated scar on the hinge
354 plate, formerly considered by Douvillé (1902) as a muscle scar, and reinterpreted by Freneix and
355 Lefrèvre (1967) as an internal ligament coupled with the resilium located between the
356 chondrophores. On the base of the hinge plate morphology *C. joannae* can be referred to the
357 subgenus *Chondrodonta* (*Freneixita*).
358 The spectacular *Chondrodonta*-bearing beds from the Cape Savudrija succession have been
359 known since the early 20th century. The material from this locality, at that time named 'Punta
360 Salvore' in the Italian language, were studied by Schubert (1903) who recognized *C. joannae*
361 (Choffat) and *C. munsoni* (Hill). This classification was predicated on the number of plicae.
362 Individuals with a greater number were referred to *C. munsoni* (Hill). However, the studied
363 specimens (Fig. 6.8) differ from the typical *C. munsoni* shells from Texas (e.g., Stanton, 1947, pl.

364 41, fig. 9) because the latter have a greater number of plicae, a more rounded crest, and a fewer
365 bifurcations. Schubert (1903) proposed three different varieties of *C. joannae*: *elongata*, *angusta*
366 and *levis*. These varieties were mostly distinguished on the basis of shell outline and ornamentation.
367 *Elongata* has a height about double that of the types of *C. joannae*. *Angusta* has a narrow shell (e.g.,
368 Fig. 6.3), with a length about half that of *elongata* (3 cm vs. 6 cm). Further, *levis* is smooth, or
369 nearly so (e.g., Figs 6.1, 6.2). All these varieties are associated in the same beds and, therefore, they
370 are here considered as ecomorphotypes of *C. joannae*, as previously proposed by Dhondt and Dieni
371 (1993, with the synonym list). A broad intraspecific morphological variability is recurrent in the
372 cemented bivalves (e.g., Harper, 2012).
373
374 **6. Functional interpretation and discussion**
375
376 *6.1. Function of the chondrophores*
377
378 The extinct family Chondrodontidae is placed within the Plicatuloidea (Carter et al., 2011), a
379 superfamily today represented only by *Plicatula*. This genus is cemented on the right valve but
380 differs from *Chondrodonta* because it has a secondary isodont hinge and an alivincular-fossate
381 ligament dorsally enclosed by the teeth (Yonge, 1973; Hautmann, 2004; Carter et al., 2012). The
382 ligament of *Plicatula* is antero-posteriorly compressed, overarching the hinge plate, inserted within
383 a deep triangular pit, and slightly asymmetrical with the right branch longer that the left one
384 (Yonge, 1973). In *Chondrodonta,* the combination of extreme ventral growth and torsion of the
385 chondrophores would have brought to the reduction of hinge. Therefore, *Chondrodonta* and
386 *Plicatula* show remarkable differences of the hinge and ligament morphologies.
387 The chondrophores are present both in attached epifaunal and deep infaunal bivalves and
388 allow the movement of the valves in different directions. Anomiacea are epifaunal byssally attached
389 bivalves, having a morphology similar to the Chondrodontidae. Both groups have essentially

edentulous shells with chondrophore-like structures. For instance, the anomiid *Pododesmus cepio* (Gray) has a convex right resilifer with a mushroom-shape and a concave left resilifer. When muscles relax the upper valve moves both laterally and dorso-ventrally (Yonge, 1973, p. 461). The deep infaunal *Mya arenaria* Linnaeus has asymmetrical chondrophores which bear a horizontally oriented ligament (Yonge, 1982). This bivalve has a hydraulic burrowing mechanism with the ejection of water through the pedal gape allowed by the movement of the valves along the dorsoventral axis (Checa and Cadée, 1997).

The elongated and interlocked chondrophores, occurring along the hinge plate of *C. joannae*, mostly acted as a hinge. The opening mechanism of the valves, which probably produced a very slight gape as already noted in *Plicatula* (Yonge, 1973), was operated by the resilium located between the chondrophores projected inside the body cavity. The opening mechanism could have been aided by the secondary ligament, if present, as suggested by Freneix and Lefrèvre (1967; Fig. 9). The possible occurrence of this secondary ligament, the tight interlocking of chondrophores in the hinge plate, the occurrence of symmetrical inner folds along the anterior and posterior regions of the attached valve and the absence of a significant lateral asymmetry of the shell, all excluded a rocking movements in the antero-posterior direction.

A slight asymmetrical elongation of chondrophores in the ventral direction could have allowed a slight movement, parallel to the commissural plane, in a dorsal-ventral direction. However, the remarkable elongation of the hinge region and the burial of the umbonal extremity should have prevented the movements in this direction. In the older species (e.g., *C. glabra* Stanton or *C. munsonii* Stanton), which have less elongated shells, and probably lacking of the secondary ligament, a lateral rocking of the valves cannot be excluded, although no morphological character seems to support this opening mechanism. Therefore, the chondrophores of *Chondrodonta* had, along the hinge plate, an alignment function among valves, as can be determined by the lack of teeth, sockets, and an outer ligament (Fig. 9). A functional ligament inside the entire hinge plate is not supported in the studied shells (Fig. 9.4). The ligament might have still been active near the

416 body cavity but, dorsally, the left blade-like chondrophore interlocks almost perfectly within the
417 socket of the right valve (Figs. 5.6, 9). This narrow interlocking could have been caused by the
418 diagenetic compaction, although the increasing of the thickness of left chondrophore, enveloped by
419 foliated calcite, suggests this to be a morphological feature which leaves little space for the
420 ligament. The appearance of a probable secondary ligament, characterizing *Chondrodonta*
421 (*Freneixita*), can be related to the size increasing and development of stick-like shells during the
422 ontogeny.

423 The most renowned extinct club- or stick-like bivalves which followed a "mud sticker"
424 strategy of stabilization on soft-bottom substrates are the Jurassic *Lithiotis* and the Cretaceous
425 *Konbostrea*. Both of these genera have short ventral body cavities and very elongated
426 dorsal/umbonal regions filled by chalky aragonite or calcite (Seilacher, 1984; Chinzei, 2013 and
427 references therein). These soft-bottom benthic bivalves had a very thin and elongated free valve
428 with the outer shell layer made by a calcitic prismatic microstructure (Chinzei, 1986). In *Lithiotis*,
429 the opening mechanism was based on the flexibility of the thin ventral margin coupled with a
430 multivincular-like ligament, which allowed small changes in the distances between the valves
431 (Savazzi, 1996). In *Konbostrea*, meanwhile, the ligament only retained its function in the juvenile
432 stage, up to a shell height of ~ 20 cm. During the adult stage, by contrast, when shells could reach
433 more than one meter in height, the valves were fused along the hinge plate and opening was
434 facilitated by the bending of the thin and flat right valve, which articulated on the fulcrum
435 represented by the ventral edge of hinge plate (Chinzei, 1986).

436 The valves of *C. joannae* do not seem to be fused together along the hinge plate. In most
437 part of the specimens, lying with the commissure parallel to the bedding plane, the inner shell
438 surfaces are often fused but this can be related to a diagenetic effect originated by the dissolution of
439 the inner aragonite layer. In some specimens buried with the commissural plane perpendicular to
440 the bedding plane, the space between the valves is filled by sediment. The tight interlocking of
441 chondrophores and the probable secondary ligament generally prevented the sediment infilling the

space between the valves. The flexibility of the shell was restricted to the ventral region of body cavity, the bending capacity of which was probably less developed than that of *Lithiotis* and *Konbostrea* due to the absence of an outer prismatic calcitic layer and a flattened free valve, and a greater shell thickness (rapidly increasing inwards). Therefore, *C. joannae* had a moderate shell flexibility of ventral margin, probably supported by a still active resilium between the chondrophores occurring in the ventral part of the hinge plate and a secondary ligament on the dorsal edges of body cavity (Fig. 9).

C. joannae developed an opening mechanism again based on the ligaments. When muscle relaxed, the extended ligament caused the opening of the ventral commissure. This mechanism acted like a nutcracker with the nut replaced by a coil spring. When the hand ceases to close the nutcracker the spring opens the handles. Following this hypothesis, the opening mechanism was mostly based on the resilium located between the chondrophores protruding in the body cavity, while the secondary ligament and interlocked chondrophores guaranteed the valve alignment.

6.2. *The club-like shell and the "mud-sticker" life strategy*

C. joannae from Cape Savudrija succession shows all the adaptations typical of a bivalve with a club-like morphology, which is characterized by strongly elongated shells which are secondarily adapted to soft-bottom substrates following a "mud sticker" stabilization strategy (Seilacher, 1984). This group contains suspension feeding and weakly-cemented bivalves, which were attached to secondary hard substrates only during the early growth stage. The shell elongation was necessary to avoid the burial of the commissure and gill suffocation caused both by the high carbonate sedimentation rate and fecal products which were trapped among the shells in low agitated shallow water benthic environments. The "mud-sticker" bivalves originated as densely crowded aggregations with strong feeding and spatial competitions as result of a high shell ecomorphism (e.g., Seilacher, 1984; Ayoub-Hannaa and Fürsich, 2011; Chinzei, 2013).

468 The shell elongation of club-like bivalves was acquired through different growth strategies
469 (Chinzei, 1982, 2013). In the relay-type, typical of *Crassostrea*, the shells grow one over the other
470 generating an upright column of individuals buried in the mud. The cone-type elongation is typical
471 of *Saccostrea* and rudists belonging to the elevator ecological category. The lower valve has a
472 cylindro-conical shape and the upper has a lid-like shape. The abandoned body cavity is chambered
473 and the upper tabula sustains the soft parts. In the konbo-type, both the valves grow vertically and,
474 to maintain the soft parts above the bottom surface, the abandoned body cavity is filled by chalky
475 deposit. This growth is typically represented by the Cretaceous *Konbostrea*, up to 130 cm in height,
476 and the Lower Jurassic pteriomorphian reaching a maximum size of about 40 cm in height (Chinzei,
477 2013).
478 The chalky deposit of *Konbostrea* is represented by calcite whereas it is aragonitic in
479 *Lithiotis* (e.g., Chinzei, 2013). In recent oysters, the chalky deposit consists of bio-induced white,
480 fibrous and highly porous material, filled by water and enclosed by foliated calcite. The chalky
481 deposits allow a lightweight strategy and a lower energetic cost in secreting shells with a fast
482 growth rates (Seilacher, 1984; Chinzei, 2013; Vermeij, 2014 and references therein). Unlike the
483 above cited konbo-type mud stickers, *C. joannae* has not chalky shell-filling material, probably
484 because its free valve had a lower flexibility and therefore needed a stronger fulcral edge. The body
485 cavity of *C. joannae* is filled by foliated calcite and a small nucleus, representing the lower
486 chondrophore, made up by homogeneous microstructure. On contrary, *Lithiotis* and *Konbostrea* had
487 very thin and flat free valves, which articulation did not need a massive fulcral edge. Therefore, the
488 hinge plate of *C. joannae* was massive because it served both as fulcrum and hinge of a shell
489 lacking valve articulation.
490 The valve alignment of *C. joannae* was mostly guaranteed by the tight interlocking of
491 chondrophores in the hinge plate. This function was probably necessary because the adult shells
492 were only partially buried and unprotected by the sediments with the most part of the shell within
493 seawater column. This supposed inclined growth habit is supported by the absence of large and

494 adult individuals with a vertical posture in all the *Chondrodonta*-bearing beds in Cape Savudrija
495 succession. Moreover, this position was necessary to maintain the flexible part of the shell, mainly
496 corresponding to the body cavity, uncovered by the sediment which otherwise would hindered the
497 shell opening movements. The shells have generally a curved commissural plane, therefore they
498 generated wide, but relatively low, bouquet-like densely crowded aggregates. While *Lithiotis* and
499 *Konbostrea* lived with prevailing upright and almost completely buried shells, *C. joannae* had
500 inclined and curved shells projected above the water-bottom interface at least for 10-20 cm,
501 originating an aggregation similar to a low shrub (Fig. 10). The body cavity of *C. joannae* might not
502 have been very far away from the sediment surface, because the suspended food increases near the
503 water-sediment interface (Chinzei, 2013; Gili and Götz, 2018). The observed bioerosion traces of
504 sponges and small boring bivalves, cannot be used to support this suggested life position because
505 the few available shells do not provide useful information on the timing and distribution of
506 bioerosion on the shell surface. It is impossible to determine if the shell was bored in life position or
507 after falling on the bottom.
508 The older *Chondrodonta* populations, occurring in the Early Cretaceous Mediterranean
509 province, are characterized by small sized and prevailing smooth shells. *C. glabra* from the early
510 Aptian of the Gargano Promontory (southern Italy) is about 10-12 cm high, has a spoon-shaped
511 shell with a very short hinge plate and a lower elongation degree (height/length ratio) than *C.*
512 *joannae* (Posenato et al., 2018). On the contrary, the latter species developed large and aberrant
513 club-like shells, which spread in the upper Cenomanian carbonate platforms (Dhondt and Dieni,
514 1993).
515 In the upper part of Cape Savudrija succession, *C. joannae* is more abundant than the
516 radiolitids. Both these bivalves were adapted to high sedimentation rates and therefore can be
517 considered within the ecological morphotype of the elevators (Skelton and Gili, 2002), although
518 their commissural plane has a different orientation.
519

520 6.3. *Early Aptian and late Cenomanian* Chondrodonta *proliferation*

521

522 *Chondrodonta* has been considered an opportunistic and r-strategist taxon (Graziano et al.,
523 2013) with a broad geographic (Middle East to Caribbean regions) and stratigraphic (Barremian to
524 Turonian) distribution. The early Aptian *C. glabra* formed in the Gargano Promontory paucispecific
525 accumulations containing a single or few generations which were rapidly buried after periodic mass
526 mortality events. These accumulations have been considered as markers of unstable environmental
527 conditions and high sedimentation processes predating the peak of the OAE 1a (Graziano, 2013;
528 Posenato et al., 2018).

529 Upper Cenomanian *C. joannae* accumulations of the Istrian Peninsula have a taphonomical
530 signature similar to the above mentioned early Aptian *C. glabra* accumulations, indicating periods
531 of high food availability and environmental instability. Sedimentological and paleontological data
532 suggest a very shallow and stressed marine setting for the *Chondrodonta* congregations of Cape
533 Savudrija succession. The upper part of the Cape Savudrija succession consists of stromatolite and
534 algae-foraminiferal limestone alternations, which can be interpreted as intertidal-subtidal cycles. A
535 stressed environment is suggested by the presence of the micro-problematicum *Thaumatoporella*,
536 nubeculariid foraminifers and possible calcimicrobe *Decastronema* sp. (e.g., Schlagintweit et al.,
537 2015 and references therein). The subtidal *Chondrodonta*-bearing unit also contains radiolitids and
538 rare monopleurids, belonging to the elevator paleoecological morphotype, typical for inner platform
539 setting (Skelton, 2003; Moro et al., 2007; Skelton and Gili, 2012; Gili and Götz, 2018).

540 The abundance of *C. joannae* and its dominance over rudists in the late Cenomanian could
541 be related to their different life habit and ecological niche. Rudists, here mostly represented by
542 radiolitids (and rare individuals of monopleurids) had a constratal mode of life because the
543 commissure projected few centimetres above the sediment-water interface (Gili et al., 1995), while
544 *C. joannae* filtered at a greater distance from the substrate (10 – 20 cm), straining towards a
545 superstratal position, similarly to the exposed framework of the hermatypic corals (Gili et al.,

546 1995). The vertical position of epifaunal suspension feeders with respect the sediment-water
547 interface has been related to the amount of re-suspended particulate organic material and the
548 thickness of benthic hydrodynamic layer (Bottjer and Ausich, 1986). These factors control the
549 resource partitioning and the tiering of epifaunal communities which, during the Cretaceous, were
550 characterized by a remarkable lowering of filtering levels (Bottjer and Ausich, 1986).
551 The constratal vs. superstratal mode of life has been also related to the climatic regime. The
552 predominant greenhouse conditions promoted the diffusion of constratal rudist-dominated
553 communities, possibly due to the frequent widespread lateral redistribution of bioclastic sediments
554 enforced by the limited increments of accommodation space, while the superstratal communities
555 would have developed during colder phases (Gili et al., 1995; Gili and Götz, 2018). Biostratigraphy
556 indicate that the thriving phase of *C. joannae* occurred during the late Cenomanian slightly before
557 the latest Cenomanian OAE 2 (Bonarelli event). This latter was characterized by severe
558 perturbation of the C-cycle, which strongly affected both terrestrial and marine ecosystems (e.g.,
559 Jenkyns et al., 2017; Bottini and Erba, 2018, Frijia et al., 2019; Laurin et al., 2019). However, also
560 the time before the OAE-2 was characterised by climatic instability with frequent temperature,
561 nutrients and other environmental fluctuations (Bottini and Erba, 2018 and reference therein;
562 O'Brien et al., 2017; Laurin et al., 2019; Schröder-Adams et al., 2019; Baker et al., 2020). In
563 particular cooling phases before the onset of the OAE 2, have been coupled with high fertility
564 episodes occurred in the oceanic domain (Bottini and Erba, 2018). This scenario would have
565 favoured opportunistic and r-strategist bivalves which had the capacity to filtering from a higher
566 part of the water column. This different tiering level and a higher amount of suspended organic
567 material would have allowed *Chondrodonta* to thrive with and partially overcome rudists during the
568 cooler phases of the late Cenomanian. This hypothesis, however, must be tested through the
569 correlation between the upper Cenomanian *Chondrodonta*-bearing beds of shallow marine
570 environment and the climatic events recognized in both shallow and deep-water environments
571 through studying other upper Cenomanian sections from different areas of the Tethyan Realm.

572

573 **7. Conclusions**

574

575 During the late Cenomanian, large areas of the Adriatic Carbonate Platform record the
576 spread of the oyster –like bivalve *C. joannae*. This bivalve originated densely-packed
577 accumulations cropping out along the rocky coast of Cape Savudrija (northern Istria, Croatia). At
578 this succession, *C. joannae* is represented by very large shells, up to 50 cm high, which developed a
579 "mud-sticker" strategy of bottom stabilization. The shell is generally curved and had an inclined
580 posture. Likewise to the other aberrant club-like bivalves, *C. joannae* developed a peculiar
581 morphology for the opening and closing shell mechanism, which was allowed by the resilium
582 located on the chondrophores projecting inside the body cavity. The valve bending and elasticity
583 were guaranteed by the ventral edge of umbonal region which robustness was sustained by the
584 filling of the body cavity with a predominant calcitic hinge platform where the modified
585 chondrophore acted as a strong hinge to guarantee the valve alignment of a shell well projected
586 above the water-sediment interface.

587 *C. joannae* had a prolific coverage rate and constructed dense and paucispecific
588 assemblages, with a low rate of generational overturning. The shells formed low-relief bivalve
589 mounds with low shrub-type congregations, partially preserved in the Cape Savudrija. The
590 dominance of *C. joannae* over rudists in the upper part of the section can be related to its ability to
591 increase the distance of the gills from the seabed. This enhanced ecological partitioning of the late
592 Cenomanian epifaunal communities could have been an advantage during high trophic and cooler
593 temperature phases, as have been recognized in deep marine settings, predating the OAE 2. Further
594 investigations are necessary to test this hypothesis, however.

595

596 **Acknowledgements**

597

We are grateful to Peter Skelton for his careful and detailed review, valuable comments and intriguing suggestions which strongly improved the manuscript. The editor Isabel Montanez and an anonymous reviewer are also deeply acknowledged. Sam Purkis is thanked for his courtesy in correcting the English. This work is a contribution to the project "Biota resilience to global change: biomineralization of planktic and benthic calcifiers in the past, present and future" supported by MURST (PRIN 2017). The research was also supported by funding provided by Ferrara University (FAR 2018 and 2019).

References

Ayoub-Hannaa, W., Fürsich, F. T., 2011. Functional morphology and taphonomy of Cenomanian (Cretaceous) oysters from the eastern Sinai Peninsula, Egypt. Palaeobiodiversity and Palaeoenvironments 91, 197–214. https://doi.org/10.1007/s12549-011-0051-7

Baker, S. J., Belcher, C. M., Barclay, R. S., Hesselbo, S. P., Laurin, J., Sageman, B. B., 2020. CO2-induced climate forcing on the fire record during the initiation of Cretaceous oceanic anoxic event 2. GSA Bulletin 132, 321–332. https://doi.org/10.1130/B35097.1.

Bieler, R., Carter, J. G., Coan, E. V., 2010. Classification of bivalve families. In P. Bouchet, J.P. Rocroi (Eds.), Nomenclator of bivalve families. Malacologia 52 (2), 1–184. https://doi.org/10.4002/040.052.0201.

Bottini, C., Erba, E., 2018. Mid-Cretaceous paleoenvironmental changes in the western Tethys. Clim. Past 14, 1147–1163. https://doi.org/10.5194/cp-14-1147-2018.

Bottjer, D. J., Ausich, W. I., 1986. Phanerozoic development of tiering in soft substrata suspension-feeding communities. Paleobiology 4, 400-420. https://doi.org/10.1017/S0094837300003134.

Brandolese, V., Posenato, R., Nebelsick, J., Bassi, D., 2019. Distinguishing core and flank facies based on shell fabrics in Lower Jurassic lithiotid shell beds. Palaeogeogr. Palaeoclimatol. Palaeoecol. 526, 1–12. https://doi.org/10.1016/j.palaeo.2019.04.010.

624 Brčić, V., Glumac, B., Fuček, L., Grizelj, A., Horvat, M., Posilović, H., Mišur, I., 2017. The
625 Cenomanian–Turonian boundary in the northwestern part of the Adriatic Carbonate Platform
626 (Ćićarija Mtn., Istria, Croatia): characteristics and implications. Facies 63 (3), 17.
627 https://doi.org/10.1007/s10347-017-0499-7.
628 Carter, J.G., 1990. Evolutionary significance of shell microstructures in the Palaeotaxodonta,
629 Pteriomorphia and Isofilibranchia (Bivalvia: Mollusca). In: Carter, J. G. (Ed.), Skeletal
630 Biomineralization: Patterns, Processes and Evolutionary Trends. vol. 1. von Nostrand
631 Reinhold, New York, pp. 135–301.
632 Carter, J. C., Altaba, C. R., Anderson, L. C., Araujo, R., Biakov, A. S., Bogan, A. E., et al., 2011. A
633 synoptical classification of the Bivalvia (Mollusca). Paleontol. Contrib. 4, 1–47.
634 Carter, J. G., Harries, P. J., Malchus, N., Sartori, A. F., Anderson, L. C., Bieler, R., Bogan, A. E.,
635 Coan, E. V., Cope, J. C. W., Cragg, S. M., García-March, J. R., Hylleberg, J., Kelley, P.,
636 Kleemann, K., Kříž, J., McRoberts, C., Mikkelsen, P. M., Pojeta Jr., J., Tëmkin, I., Yancey,
637 T., Zieritz, A., 2012. Part N, Revised, Volume 1, Chapter 31: Illustrated Glossary of the
638 Bivalvia. Treatise Online 48, 1–209.
639 Cazzini, F., Zotto, O. D., Fantoni, R., Ghielmi, M., Ronchi, P., Scotti, P., 2015. Oil and Gas in the
640 Adriatic foreland, Italy. J. Pet. Geol. 38 (3), 255–279. https://doi.org/10.1111/jpg.12610.
641 Checa, A., Cadée, G. C., 1997. Hydraulic burrowing in the bivalve *Mya arenaria* Linnaeus
642 (Myoidea) and associated ligamental adaptations. J. Moll. Stud. 63(2), 157–171.
643 https://doi.org/10.1017/S0025315400038753.
644 Chinzei, K., 1982. Morphological and structural adaptations to soft substrates in the Early Jurassic
645 monomyarians *Lithiotis* and *Cochlearites*. Lethaia 15, 179–197.
646 https://doi.org/10.1111/j.1502-3931.1982.tb01137.x.
647 Chinzei, K., 1986. Shell structure, growth, and functional morphology of an elongate Cretaceous
648 oyster. Palaeontology 29(1), 139–154.

649 Chinzei, K., 2013. Adaptation of oysters to life on soft substrates. Historical Biology 25(2), 1–9.
650 https://doi.org/10.1080/08912963.2012.727412.
651 Chiocchini, M., Pampaloni, M.L., Pichezzi, R.M., 2012. Microfacies e microfossili delle
652 successioni carbonatiche mesozoiche del Lazio e dell'Abruzzo (Italia centrale): Cretacico.
653 Mem. Carta Geol. d'Italia 17, 269 pp.
654 Cox, L. R., Stenzel, H. B., 1971. Families doubtfully related to oysters. Family Chondrodontidae
655 Freneix, 1959. In: Moore, R.C. (Ed.), Treatise on Invertebrate Paleontology, Part N, Vol. 3 (of
656 3) Mollusca 6, Bivalvia 1197–1200.
657 Dalla Vecchia, F.M., Tarlao, A., Tunis, G., Venturini, S., 2001. Dinosaur track sites in the Upper
658 Cenomanian (Late Cretaceous) of Istrian peninsula (Croatia). B. Soc. Paleont. Ital. 40, 25–54.
659 Davey, S. D., Jenkyns, H. C., 1999. Carbon-isotope stratigraphy of shallow-water limestones and
660 implications for the timing of Late Cretaceous sea-level rise and anoxic events (Cenomanian-
661 Turonian of the peri-Adriatic carbonate platform, Croatia). Eclogae Geol. Helv. 92, 163–170.
662 Dhondt, A. V, Dieni, I., 1992. Non-rudistid bivalves from Cretaceous rudist formation. Geol. Rom.
663 28, 211–218.
664 Dhondt, A.V., Dieni, I., 1993. Non-rudist bivalves from Late Cretaceous rudist limestones of the
665 NE Italy (Col dei Schiosi and Lago di S. Croce areas). Sci. Geol. Mem. 45, 165–241.
666 Douvillé, H., 1902. Sur le genre *Chondrodonta* Stanton. Bull. Soc. Géol. Fr. 4e Sér, vol. T2, 314–
667 318.
668 Freneix, S., Lefèvre, R., 1967. Deux espèces nouvelles de *Chondrodonta* et *Neithea* (Bivalves) du
669 Sénonien du Taurus lycien (Turquie). Bull. Soc. Géol. Fr. 9 (7), 762–776.
670 https://doi.org/10.2113/gssgfbull.S7-IX.5.762.
671 Frijia, G., Parente, M., Di Lucia, M., Mutti, M., 2015. Carbon and strontium isotope stratigraphy of
672 the Upper Cretaceous (Cenomanian-Campanian) shallow-water carbonates of southern Italy:
673 Chronostratigraphic calibration of larger foraminifera biostratigraphy. Cretaceous Res. 53,
674 110–139. https://doi.org/10.1006/cres.2002.1017.

675 Frijia, G., Forkner, R., Minisini, D., Pacton, M., Struck, U., Mutti, M., 2019. Cyanobacteria
676 Proliferation in the Cenomanian-Turonian Boundary Interval of the Apennine Carbonate
677 Platform: Immediate Response to the Environmental Perturbations Associated With OAE2?
678 Geochemistry, Geophys. Geosystems 20, 2698–2716.
679 https://doi.org/10.1029/2019GC008306.
680 Gili, E., Götz, S., 2018. Part N, Revised, Volume 1, Chapter 26B: Paleoecology of Rudists. Treatise
681 Online 103, 1–29. https://doi.org/10.17161/to.v0i0.7183.
682 Gili, E., Masse, J.-P., Skelton, P.W., 1995. Rudists as gregarious sediment-dwellers, not
683 reefbuilders, on Cretaceous carbonate platforms. Palaeogeogr. Palaeoclimatol. Palaeoecol.
684 118, 245–267. https://doi.org/10.1016/0031-0182(95)00006-X.
685 Grandić, S., Kratkoviæ, I., Baliæ, D., 2013. Peri-Adriatic platforms Proximal Talus reservoir
686 potential (part 1). Nafta 64, 147–160.
687 Graziano, R., 2013. Sedimentology, biostratigraphy and event stratigraphy of the early Aptian
688 Oceanic Anoxic Event (OAE1A) in the Apulia Carbonate Platform Margin - Ionian Basin
689 System (Gargano Promontory, southern Italy). Cretaceous Res. 39, 78–111.
690 https://doi.org/10.1016/j.cretres.2012.05.014.
691 Graziano, R., Raspini, A., Spalluto, L., 2013. High resolution δ 13C stratigraphy through the Selli
692 Oceanic Anoxic Event (OAE1a) in the Apulia carbonate platform: the Borgo Celano section
693 (western Gargano Promontory, Southern Italy). Ital. J. Geosci. 132 (3), 477–496.
694 https://doi.org/10.3301/IJG.2013.16.
695 Guerzoni, S., 2016. Analisi delle facies di piattaforma interna del Promontorio del Gargano
696 nell'intervallo Barremiano superiore - Aptiano inferiore e confronto con le piattaforme tetidee
697 durante l'Evento Anossico OAE1a (PhD thesis). Univ. Ferrara, 294 pp.
698 Gušić, I., Jelaska, V., 1990. Stratigrafija gornjokrednih naslaga otoka Brača u okviru geodinamske
699 evolucije Jadranske karbonatne platforme [Upper Cretaceous stratigraphy of the Island of

Brač within the geodynamic evolution of the Adriatic carbonate platform (in Croatian and English). Djela Jugoslavenske akademije znanosti i umjetnosti 69, JAZU-IGI, Zagreb, 160 pp.

Gušić, I., Jelaska, V., 1993. Upper Cenomanian-lower Turonian sea-level rise and its consequences on the Adriatic-Dinaric carbonate platform. Geol. Rundschau 82, 676–686. https://doi.org/10.1007/BF00191495.

Harper, E. M., 2012. Part N, Revised, Volume 1, Chapter 21: Cementing Bivalvia. Treatise online 45, 1-12. https://doi.org/10.17161/to.v0i0.4276

Hautmann, M., 2004. Early Mesozoic evolution of alivincular bivalve ligaments and its implications for the timing of the 'Mesozoic marine revolution'. Lethaia 37(2), 165–172. https://doi.org/10.1080/00241160410005835.

Herak, M., 1991. Dinaridi-mobilistički osvrt na genezu I strukturu (Dinarides-mobilistic view of the genesis and structure). Acta Geologica 21, 35-117.

Hoernes, R., 1902. *Chondrodonta* (*Ostrea*) *Joannae* Choffat in den Schiosischichten von Görz, Istrien, Dalmatien und der Herzegowina. Sitzungsber. d. kais. Akad. d. Wissensch. Wien, math.-naturw. Cl. 111, 667–684.

Jenkyns, H. C., 1991. Impact of Cretaceous sea level rise and anoxic events on the Mesozoic carbonate platform of Yugoslavia. Am. Assoc. Pet. Geol. Bull. 75, 1007–1017.

Jenkyns, H. C., Dickson, A. J., Ruhl, M., van den Boorn, S.H. J. M., 2017. Basalt–seawater interaction, the Plenus Cold Event, enhanced weathering and geochemical change: deconstructing Oceanic Anoxic Event 2 (Cenomanian–Turonian, Late Cretaceous). Sedimentology 64, 16–43. https://doi.org/10.1111/sed.12305.

Jurkovšek, B., Tolman, M., Ogorelec, B., Šribar, L., Drobne, K., Poljak, M., Šribar, L., 1996. Formacijska geološka karta južnega dela Tržaško-Komenske planote. Kredne in paleogenske karbonatne kamine (Geological map of the southern part of Trieste-Komen plateau. Cretaceous and Paleogene carbonate rocks (In Sloveniana and English), Inštitut za geologijo, geotehniko in geofiziko, Ljubljana, 143 pp.

726 Korbar, T., 2009. Orogenic evolution of the External Dinarides in the NE Adriatic region: a model
727 constrained by tectonostratigraphy of Upper Cretaceous to Paleogene carbonates. Earth-
728 Science Rev. 96, 296–312. https://doi.org/10.1016/j.earscirev.2009.07.004.
729 Korbar, T., Glumac, B., Tesovic, B. C., Cadieux, S. B., 2012. Response of a carbonate platform to
730 the Cenomanian-Turonian Drowning and OAE 2: a case study from the Adriatic Platform
731 (Dalmatia, Croatia). J. Sediment. Res. 82, 163–176. https://doi.org/10.2110/jsr.2012/17.
732 Laurin, J., Barclay, R. S., Sageman, B. B., Dawson, R. R., Pagani, M., Schmitz, M., Eaton, J.,
733 McInerney, F. A., McElwain, J. C., 2019. Terrestrial and marginal-marine record of the mid-
734 Cretaceous Oceanic Anoxic Event 2 (OAE 2): High-resolution framework, carbon isotopes,
735 CO2 and sea-level change. Palaeogeogr. Palaeoclimatol. Palaeoecol. 524, 118–136.
736 https://doi.org/10.1016/j.palaeo.2019.03.019.
737 Magaš, N., 1968. Osnovna geološka karta SFRJ 1:100000, List Cres L33-113 (Basic geological
738 map of SFRY: Sheet Cres L33-113). Institut za geološka istraživanja Zagreb (1965), Savezni
739 geološki istitut Beograd.
740 Márton, E., Ćosović, V., Moro, A., Zvocak, S., 2008. The motion of Adria during the Late Jurassic
741 and Cretaceous: New paleomagnetic results from stable Istria. Tectonophysics 454, 44–53.
742 https://doi.org/10.1016/j.tecto.2008.04.002.
743 Márton, E., Ćosović, V., Moro, A., 2014. New stepping stones, Dugi otok and Vis islands, in the
744 systematic paleomagnetic study of the Adriatic region and their significance in evaluations of
745 existing tectonic models. Tectonophysics 611,141–154.
746 https://doi.org/10.1016/j.tecto.2013.11.016
747 Masse, J., Steuber, T., 2007. Strontium isotope stratigraphy of Early Cretaceous rudist bivalves. In:
748 Scott R.W. (Ed.), Cretaceous Rudists and Carbonate Platforms: Environmental Feedback.
749 SEPM Special Publication 87, 159–165.
750 Mezga, A., Tunis, G., Moro, A., Tarlao, A., Ćosović, V., Bucković, D., 2006. A new dinosaur
751 tracksite in the Cenomanian of Istria, Croatia. Riv. Ital. Paleont. S. 112, 435–445.

752 Moro, A., 1997. Stratigraphy and paleoenvironments of rudist biostromes in the Upper Cretaceous
753 (Turonian-upper Santonian) limestones of southern Istria, Croatia. Palaeogeogr.
754 Palaeoclimatol. Palaeoecol. 131, 113–131. https://doi.org/10.1016/S0031-0182(96)00144-7.
755 Moro, A., Skelton, P. W., Ćosović, V., 2002. Palaeoenvironmental setting of rudists in the Upper
756 Cretaceous (Turonian–Maastrichtian) Adriatic Carbonate Platform (Croatia), based on
757 sequence stratigraphy. Cretaceous Res. 23, 489–508. https://doi.org/10.1006/cres.2002.1017.
758 Moro, A., Tunis, G., Mezga, A., Tarlao, A., Ćosović, V., 2007. Depositional Environments of the
759 Upper Cenomanian limestones with rudists and dinosaur footprints, Istria, Croatia. In:
760 Scott R.W. (Ed.), Cretaceous Rudists and Carbonate Platforms: Environmental Feedback.
761 SEPM Special Publication 87, 37–44.
762 Nevesskaja, L. A., Skarlato, O. A., Starobogatov, Ya. I., Eberzin, A. G., 1971. A new concept of the
763 bivalve system. Paleontol. Zh. 2, 3–20 (in Russian).
764 O'Brien, C. L., Robinson, S. A., Pancost, R. D., Damsté, J. S. S., Schouten, S., Lunt, D. J., Alsenz,
765 H., Bornemann, A., Bottini, C., Brassell, S. C., Farnsworth, A., Forster, A., Huber, B. T.,
766 Inglis, G. N., Jenkyns, H. C., Linnert, C., Littler, K., Markwick, P., McAnena, A., Mutterlose,
767 J., Naafs, B. D. A., Püttmann, W., Sluijs, A., van Helmond, A. G. M., Vellecoop, J., Wagner,
768 T. and Wrobel, N. E., 2017. Cretaceous sea-surface temperature evolution: Constraints from
769 TEX86 and planktonic foraminiferal oxygen isotopes. Earth-Sci. Rev. 172, 224–247,
770 https://doi.org/10.1016/j.earscirev.2017.07.012
771 Otoničar, B., 2007. Upper Cretaceous to Paleogene Forbulge Unconformity Associated With
772 Foreland Basin Evolution (Kras, Matarsko Podolje and Istria; SW Slovenia and NW Croatia).
773 Acta Carsologica 36, 101–120. https://doi.org/10.3986/ac.v36i1.213.
774 Philip, J., Airaud-Crumiere, C., 1991. The demise of the rudist-bearing carbonate platforms at the
775 Cenomanian/Turonian boundary: a global control. Coral Reefs 10, 115–125.

776 Pleničar, M., Polšak, A., Šikić, D. 1969. Osnovna geološka karta SFRJ 1:100000, List Trst L33-88
777 (Basic geological map of SFRY: Sheet Trieste L33-88). Geološki zavod, Ljubljana, Institut za
778 geološka istraživanja Zagreb (1951-1964), Savezni geološki istitut Beograd.
779 Polšak, A., 1965. Geologija južne Istre s osobitim obzirom na biostratigrafiju krednih naslaga
780 [Géologie de l'Istrie méridionale spécialement par rapport a la biostratigraphie des couches
781 crétacées]. Geološki Vjesnik 18, 415–509.
782 Polšak, A., 1967a. Kredna makrofauna južne Istre [Macrofaune crétacée de l'Istrie méridionale,
783 Yugoslavie]. Palaeontologia Jugoslavica 8, 1–219.
784 Polšak, A., 1967b. Osnovna geološka karta SFRJ, List Pula, 1:100000, L33-112 (Basic geological
785 map of SFRY: Sheet Pula L33–112). Institut za geološka istraživanja, Zagreb, Savezni
786 geološki zavod, Beograd.
787 Polšak, A., Šikić, D., 1969. Osnovna geološka karta SFRJ 1:100 000. List Rovinj L33-100 (Basic
788 geological map of SFRY: Sheet Rovinj L33–100j). Institut za geološka istraživanja, Zagreb
789 (1958-1963), Savezni geološki zavod, Beograd.
790 Posenato R., Masetti, D., 2012. Environmental control and dynamics of Lower Jurassic bivalve
791 build-ups in the Trento Platform (Southern Alps, Italy). Palaeogeogr. Palaeoclimatol.
792 Palaeoecol. 361–362, 1–13. https://doi.org/10.1016/j.palaeo.2012.07.001
793 Posenato, R., Morsilli, M., Guerzoni, S., Bassi, D., 2018. Palaeoecology of *Chondrodonta*
794 (Bivalvia) from the lower Aptian (Cretaceous) Apulia Carbonate Platform (Gargano
795 Promontory, southern Italy). Palaeogeogr. Palaeoclimatol. Palaeoecol. 508, 188–201.
796 https://doi.org/10.1016/j.palaeo.2018.08.002.
797 Ross, D. J., Skelton, P. W., 1993. Rudist formations of the Cretaceous: a palaeoecological,
798 sedimentological and stratigraphical review. Sedimentology Review 1, 73–91.
799 Savazzi, E., 1996. Preserved ligament in the Jurassic bivalve *Lithiotis*: adaptive and evolutionary
800 significance. Palaeogeogr. Palaeoclimatol. Palaeoecol. 120, 281–289.
801 https://doi.org/10.1016/0031-0182(95)00044-5.

802 Schlagintweit, F., Kołodziej, B., Qorri, A., 2015. Foraminiferan-calcimicrobial benthic
803 communities from Upper Cretaceous shallow-water carbonates of Albania (Kruja Zone).
804 Cretaceous Res. 56, 432–446. https://doi.org/10.1007/s10347-006-0100-2.
805 Schröder-Adams, C. J., Herrle, J. O., Selby, D., Quesnel, A., Froude, G., 2019. Influence of the
806 high Arctic igneous province on the Cenomanian/Turonian boundary interval, Sverdrup
807 Basin, High Canadian Arctic. Earth Planet. Science Lett. 511, 76– 88.
808 https://doi.org/10.1016/j.epsl.2019.01.023.
809 Schubert, R. J., 1903. Ueber einige Bivalven des istrodalmatinischen Rudistenkalkes. Jahr. d. k. k.
810 geol. Reich. 52 (2), 265–276.
811 Seilacher, A., 1984. Constructional morphology of bivalves evolutionary pathways in primary
812 versus secondary soft dwellers. Palaeontology 27, 207–237.Skelton, P. W., ed. 2003. The
813 Cretaceous World. The Open University and Cambridge University Press. Cambridge, UK.,
814 360 pp.
815 Skelton, P. W., 2018. Part N, Volume 1, Chapter 26A: Introduction to the Hippuritida (rudists):
816 Shell structure, anatomy, and evolution. Treatise Online 104, 1–37.
817 https://doi.org/10.17161/to.v0i0.7414.
818 Skelton, P. W., Gili, E., 2002. Paleoecological classification of rudist morphotypes . In M. S.
819 Trifunović, (Ed.), Proceedings First International Conference on Rudists (Beograd, 1988),
820 “Rudists,” Union of Geological Societies of Yugoslavia, Mem. Publ. 265–285.
821 Skelton, P. W., Gili, E., 2012. Rudists and carbonate platforms in the Aptian: a case study on biotic
822 interactions with ocean chemistry and climate. Sedimentology 59, 81–117.
823 https://doi.org/10.1111/j.1365-3091.2011.01292.x.
824 Stanton, T. W., 1901. *Chondrodonta*, a new genus of ostreiform mollusks from the Cretaceous, with
825 descriptions of the genotype and a new species. Nat. Mus. Proc. vol. 24, Smithson. Inst., US,
826 301–307. https://doi.org/10.5479/si.00963801.24-1257.301.

827 Stanton, T. W., 1947. Studies of some Comanche pelecypods and gastropods. In: USGS Prof. Pap.
828 vol. 221, 256 pp.
829 Steuber, T., Scott, R. W., Mitchell, S. F., Skelton, P. W., 2016. Part N, Revised, Volume 1, Chapter
830 26C: Stratigraphy and diversity dynamics of Jurassic–Cretaceous Hippuritida (rudist
831 bivalves). Treatise Online no. 81, 1–17. https://doi.org/10.17161/to.v0i0.6474.
832 Šikić, D., Polšak, A., Magaš, N. 1969. Osnovna geološka karta SFRJ, 1:100000, List Labin L33-
833 101 (Basic geological map of SFRY: Sheet Labin L33–101). Institut za geološka istraživanja,
834 Zagreb (1958-1967), Savezni geološki zavod, Beograd.
835 Šikić, D., Pleničar, M., Šparica, M. 1972. Osnovna geološka karta SFRJ, 1:100000, List Ilirska
836 Bistrica L33-89 (Basic geological map of SFRY: Sheet Ilirska Bistrica L33–89). Institut za
837 geološka istraživanja, Zagreb, Geološki zavod Ljubljana (1958-1967), Savezni geološki
838 zavod, Beograd.
839 Tišljar, J., Velić I., Radovčić, J., Crnković, B., 1983. Upper Jurassic and Cretaceous peritidal,
840 lagoonal, shallow marine and perireefal carbonate sediments of Istria. In: Babić, Lj., Jelaska,
841 V. (Eds.), Contributions to Sedimentology of some carbonate and clastic units of the coastal
842 Dinarides: Excursion Guide-book, 13–35, 4th IAS Regional Meeting, Split.
843 Tišljar, J., Vlahović, I., Velić, I., Sokač, B., Tisljar, J., Vlahovic, I., Velic, I., Sokac, B.,
844 Anonymous, 2002. Carbonate platform megafacies of the Jurassic and Cretaceous deposits of
845 the Karst Dinarides. Geol. Croat. 55, 139–170. https://doi.org/10.4154/GC.2002.14.
846 Velić, I., 2007. Stratigraphy and palaeobiogeography of Mesozoic benthic foraminifera of the Karst
847 Dinarides (SE Europa). Geologia Croatica 60, 1–113.
848 Velić, I., Tišljar, J., Vlahović, I., Matičec, D., Bergant, S., 2003. Evolution of the Istrian Part of the
849 Adriatic Carbonate Platform from the Middle Jurassic to the Santonian and Formation of the
850 Flysch Basin During the Eocene : Main Events and Regional Comparison. 22nd IAS Meet.
851 Sedimentol. - Opatija 2003, Field Trip Guidebook.

852 Velić, I., Malvić, T., Cvetković, M., Velić, I., 2015. Stratigraphy and petroleum geology of the
853 Croatian part of the Adriatic Basin. J. Pet. Geol. 38, 281–300.
854 https://doi.org/10.1111/jpg.12611.
855 Vermeij, G. J., 2014. The oyster enigma variations: a hypothesis of microbial calcification.
856 Paleobiology 40 (1), 1–13. http://dx.doi.org/10.1666/13002.
857 Vlahović, I., Tišljar, J., Velić, I., Matičec, D., Vlahovic, I., Tisljar, J., Velic, I., Maticec, D., 2005.
858 Evolution of the Adriatic Carbonate Platform: Palaeogeography, main events and depositional
859 dynamics. Palaeogeogr. Palaeoclimatol. Palaeoecol. 220, 333–360.
860 https://doi.org/10.1016/j.palaeo.2005.01.011.
861 Winterer, E. L. L., Bosellini, A., 1981. Subsidence and sedimentation on Jurassic passive
862 continental margin, Southern Alps, Italy. Am. Assoc. Pet. Geol. Bull. 65, 394–421.
863 Wrigley, R., Hodgson, N., Esestime, P., 2015. Petroleum geology and hydrocarbon potential of the
864 Adriatic Basin, offshore Croatia. J. Pet. Geol. 38, 301–316. https://doi.org/10.1111/jpg.12612.
865 Yonge, C. M., 1973. Functional morphology with particular reference to hinge and ligament in
866 Spondylus and Plicatula and a discussion on relations within the superfamily Pectinacea. Phil.
867 Trans. R. Soc. London. S. B, Biol. Sci. 267(883), 173–208.
868 Yonge, C. M., 1982. Ligamental structure in Mactracea and Myacea (Mollusca: Bivalvia). J. mar.
869 biol. Ass. U. K. 62(1), 171–186. https://doi.org/10.1017/S0025315400020191.
870 Zappaterra, E., 1994. Source-rock distribution model of the Periadriatic region. Am. Assoc. Pet.
871 Geol. Bull. 78, 333–354. https://doi.org/10.1306/BDFF90A0-1718-11D7-
872 8645000102C1865D.
873
874
875
876
877

878

879

880

881 Figure Captions

882

883 Fig. 1A. Geographic location of the Cape Savudrija studied area (Istria, Croatia); Fig. 1B.
884 Schematic geological map of NW Istria; legend: J3 (2-3), Kimmeridgian-Tithonian; K1 (1),
885 Valanginian; K1 (2), Hauterivian; K1 (3, 4), Barremian-Aptian; K1 (5), Albian; K2 (1),
886 Cenomanian; K2 (2), Turonian; E1, 2, lower to middle Eocene; E2, 3, middle to upper Eocene; Q,
887 Quaternary.
888 Fig. 1C, detailed geographical position of the Cape Savudrija outcrop; Fig. 1D, the lower part of the
889 Cape Savudrija succession (upper Cenomanian); Fig. 1E, the upper part of the succession (upper
890 Cenomanian, see Fig. 2) with two *Chondrodonta* mounds (Co) showing a topographic relief of few
891 decimetres.

892

893 Fig. 2. Stratigraphic column of the Cape Savudrija section (Istria, Croatia). Three different larger
894 bivalve communities have been distinguished: a) rudist communities without *Chondrodonta* shells
895 (beds R1–R3); b) rudist and *Chondrodonta* community with rare *Chondrodonta* shells (beds R4–
896 R13); *Chondrodonta*-dominated communities with subordinate rudists mainly represented by
897 radiolitids (beds R14–R25). All the photographs of the outcrops are horizontal with respect the
898 bedding.

899

900 Fig. 3. The *Chondrodonta* accumulation of bed R21. Fig. 3.1, bedding surface. Fig. 3.2, the arrows
901 indicate the position, size and growth direction of *Chondrodonta* shells. Fig. 3.3, the rose diagram
902 indicates the shell growth direction occurring on the whole surface, calculated on straight segment
903 indicated in Fig. 3.4a-d, with no reference to the arrow lengths. Fig. 3.4a-d, the rose diagrams have

been plotted for each sector in which the *Chondrodonta*-bearing surface has been divided, with no reference to the arrow lengths; the straight segments were obtained by joining the apex and the end of each arrow drawn in Fig. 3.2.

Fig. 4. Inner surface of a *Chondrodonta* shell (4A) and its mould reproduced by the mudstone (bed R24). The "inner growth lines" occurring on the internal surface of the calcitic layer (arrow) have been produced by the dissolution of the inner aragonitic layer before the complete sediment induration.

Fig. 5. Acetate peels and interpretative reconstruction of some selected sections of *Chondrodonta joannae* (Choffat), Cape Savudrija; all the sections are perpendicular to the commissural plane and anterior-posteriorly oriented. Figs 5.1, 5.2, specimen no. 1, the sections are respectively placed at a distance of about 17 cm and 13 cm from the apex of a moderately compressed shell, about 22 cm high (see Fig. 7). Fig. 5.3, specimen no. 2, section of the hinge plate located at 5.5 cm from the apex of a strongly compressed shell, 12.5 cm high (see Fig. 6.5); legend: yellow, sparry calcite cements filling the voids produced by the aragonite dissolution; light blue, the chondrophores enveloped by the foliated calcite. Fig. 5.4, section of the hinge plate of the specimen no. 3 oriented with the commissural plane perpendicular to the bedding surface; the section is located in the dorsal part of the hinge plate of a shell about 30 cm high. Figs 5.5, 5.6, outline of the section and tentative reconstruction of the un-deformed shell.

Fig. 6. *Chondrodonta joannae* (Choffat), upper Cenomanian limestone of Cape Savudrija (Istria, Croatia). Fig. 6.1, a smooth shell with the outer calcitic layer partially eroded and with prominent inner marginal ridges (bed R24). Fig. 6.2, an incomplete shell with very small bioerosion traces (arrows, bed R17). Figs 6.3– 6.9, shells with different ornamentation patterns and elongation degree (same order as photo succession, beds R19, R24, R21, R24, R19, R24, R24). Fig. 6.10, a cluster of

930 large shells with a hook-like umbonal region probably buried close to their original site of
931 cementation (bed R21); Figs 6.11, 6.12, very large shells of specimens respectively oriented with
932 the commissure plane parallel or perpendicular to the bedding surface (bed R21). Figs 6.13 (bed
933 R16) and 6.14 (bed R19), two bouquet-like congregations of juvenile specimens. All the photos,
934 except those of Figs 3-5, are from the field; the scale bar is 2 cm.
935
936 Fig. 7. *Chondrodonta joannae* (Choffat), upper Cenomanian limestone of Cape Savudrija (bed R24,
937 Istria, Croatia). For each section a scanned image and its interpretative drawing are shown. Sections
938 1.5a–1.4.3b are through the body cavity; sections 1.4.2b–1.1b are through the hinge platform. The
939 white line indicates the dorsal limit of the body cavity (BC). All the sections have the free valve on
940 the top.
941
942 Fig. 8. Internal characters of isolated valves or eroded shells of *Chondrodonta joannae* (Choffat),
943 upper Cenomanian limestone of Cape Savudrija (Istria, Croatia). Figs 8.1 and 8.8, a shell with
944 broken and almost completely eroded free valve (bed R21); the anterior ridge (R2) of the attached
945 valve is exposed while the groove (G) below the lower chondrophore is filled by fragments of the
946 free valve. Fig. 8.2, a probable large and disarticulated free valve of a strongly elongated shell,
947 about 30 cm high, with a small body cavity, about 5 cm high, indicated by the dashed red line (bed
948 R21). Figs 8.3, 8.9, the internal surface of a moderately elongated attached valve and detail of the
949 hinge plate (bed R. 23). Figs 8.4, 8.5, 8.7 internal surfaces of attached valves with the hinge plate
950 (bed R23). Figs 8.6 and 8.10, a very elongated shell with the free valve eroded in the middle part;
951 the surface of the hinge plate is well detectable (bed R19). All the photos, except that of Fig. 6, are
952 from the field; the scale bar is 5 cm.
953
954 Fig. 9. Morphology and orientation of *Chondrodonta joannae* (Choffat) from the upper
955 Cenomanian limestone of Cape Savudrija (Istria, Croatia). Figs 9.1, 9.2, position and shape of the

956 adductor muscle scar are tentative. The morphology of the inner surface of left valve is unknown,
957 because the inner shell layer was aragonitic. The occurrence of the secondary ligament follows the
958 hypothesis of Freneix and Lefrèvre (1967). The red lines delimit the hinge plate. Fig. 9.3, detail of
959 the anterior-posterior section through the chondrophores projected inside the body cavity. Fig. 9.4,
960 detail of an anterior-posterior section through the anterior side of hinge plate; the occurrence of an
961 active ligament inside the hinge plate is not supported in the study shells (see the text for
962 discussion). Abbreviations: ant.-post., anterior-posterior; chondro., chondrophore; G, groove; R,
963 ridge (for the numbers see Fig. 8);
964
965 Fig. 10. Reconstruction of *Chondrodonta joannae* (Choffat) in life position forming a bouquet-like
966 congregation similar to a low shrub. For comparison, a radiolitid bouquet at the right.

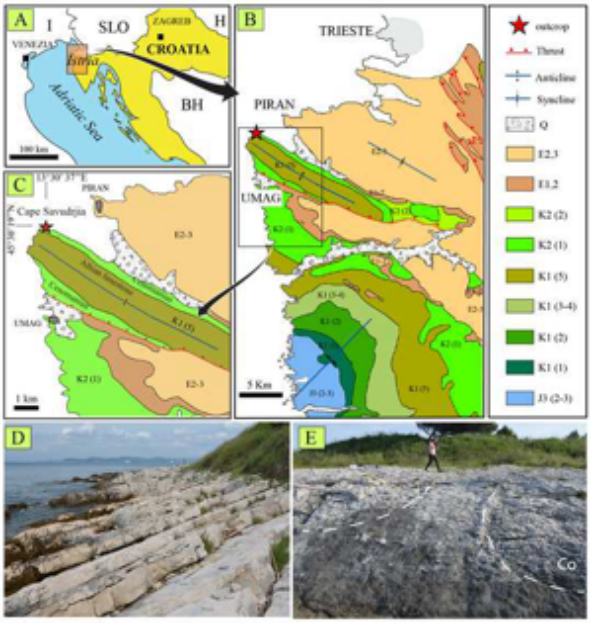

Figure 1

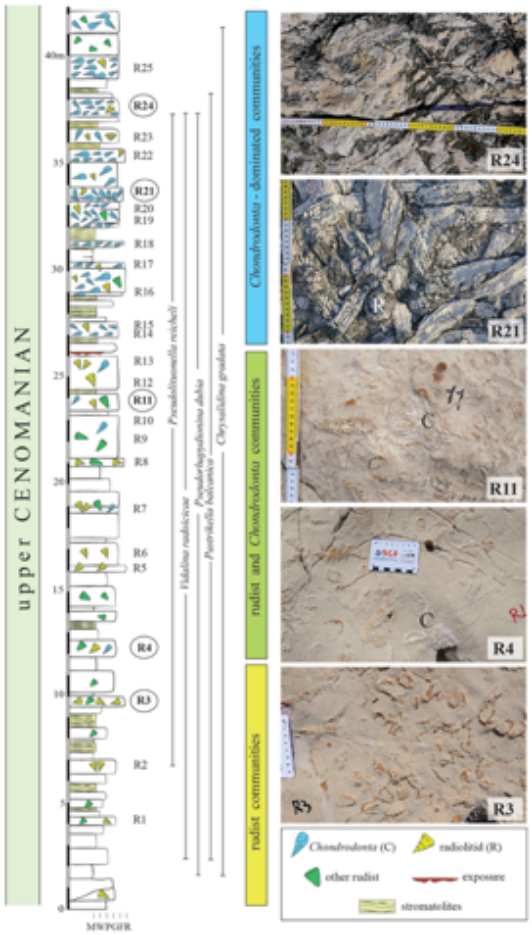

Figure 2

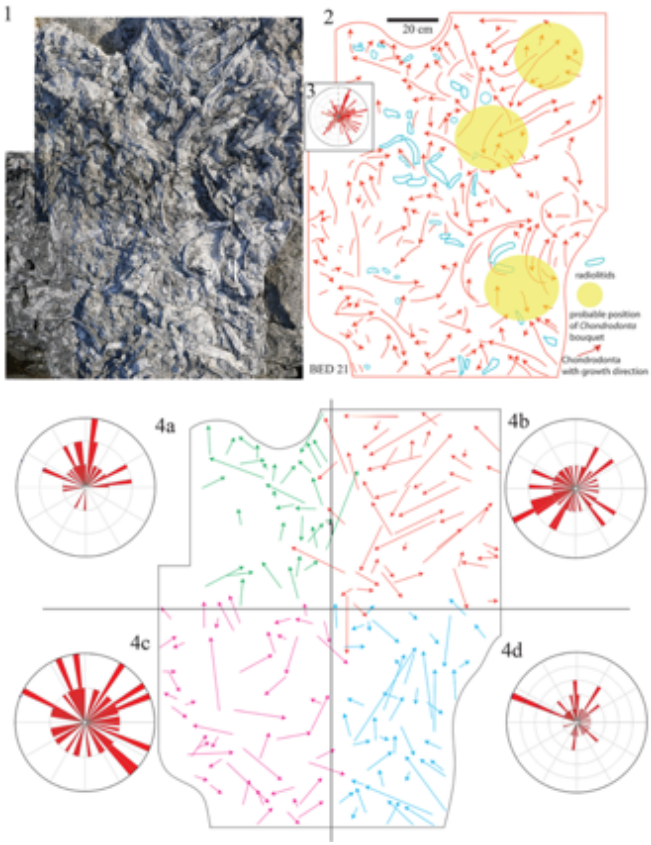

Figure 3

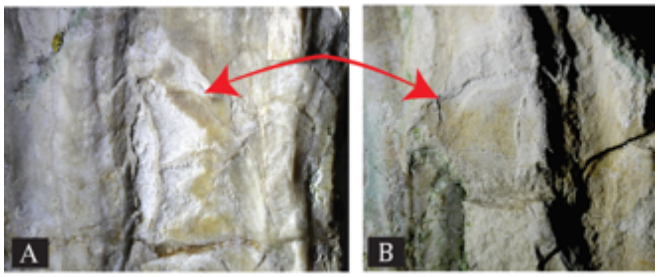

Figure 4

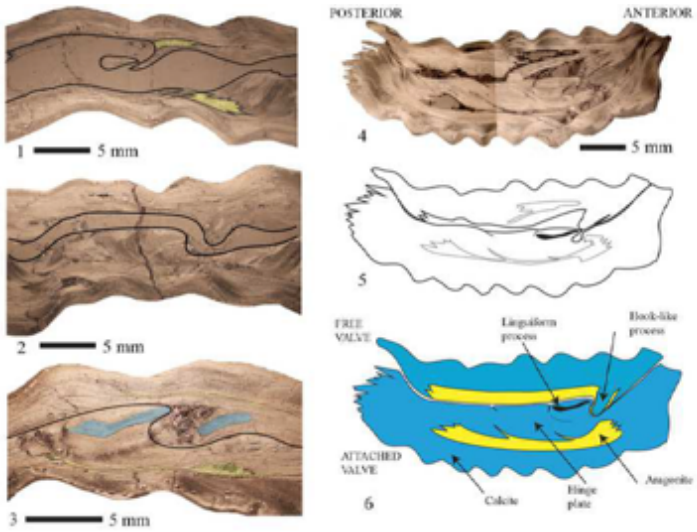

Figure 5

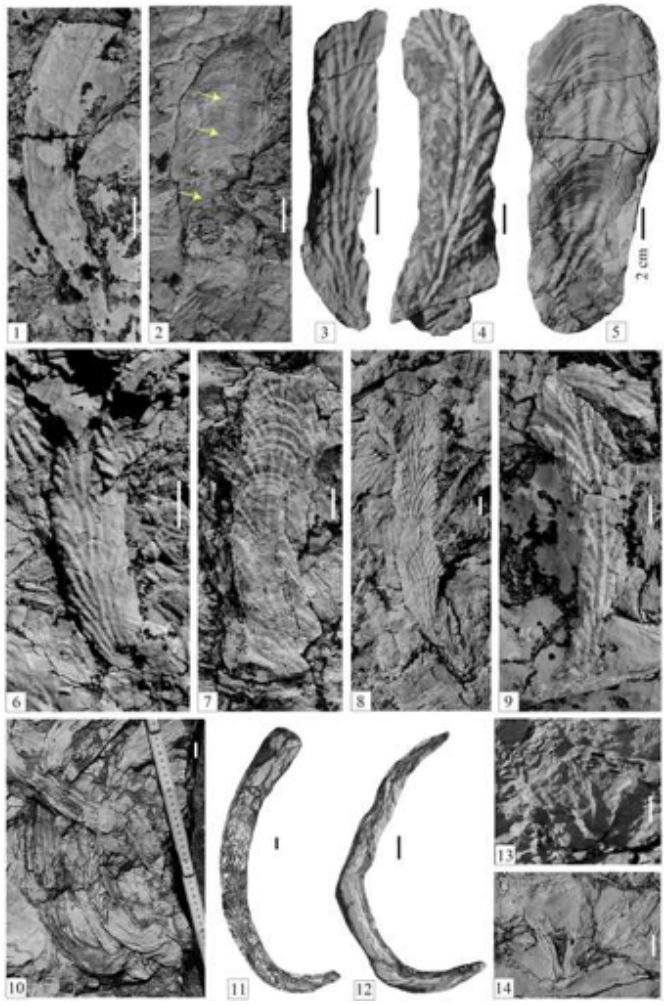

Figure 6

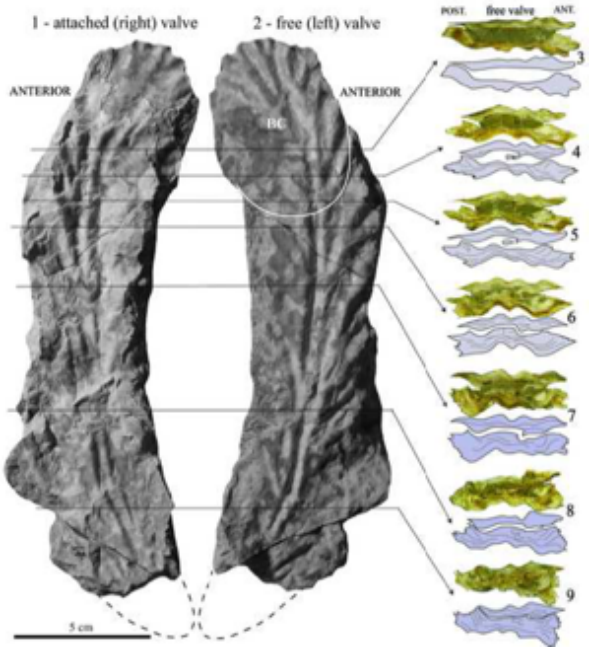

Figure 7

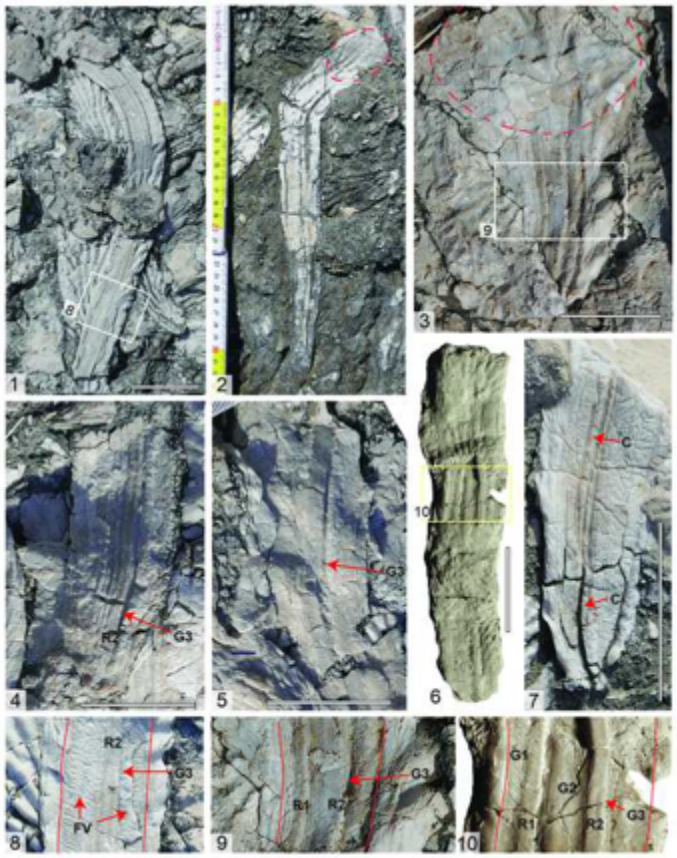

Figure 8

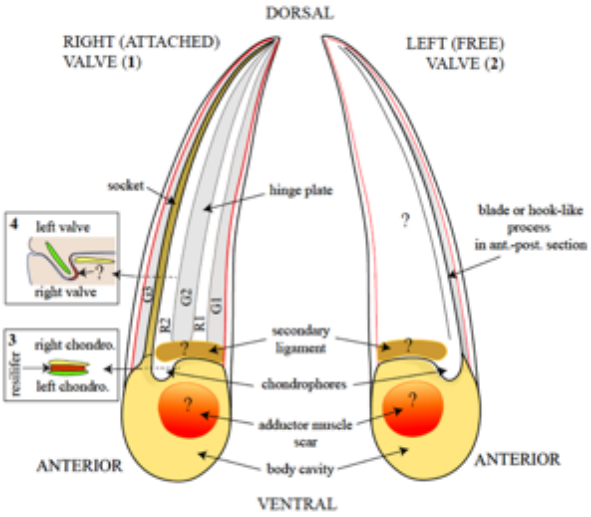

Figure 9

Figure 10